



Deposited via The University of Leeds.

White Rose Research Online URL for this paper:

<https://eprints.whiterose.ac.uk/id/eprint/84216/>

Version: Accepted Version

Article:

Grant, ER, Ross, AN, Gardiner, BA et al. (2015) Field observations of canopy flows over complex terrain. *Boundary-Layer Meteorology*, 156 (2). pp. 231-251. ISSN: 0006-8314

<https://doi.org/10.1007/s10546-015-0015-y>

Reuse

Items deposited in White Rose Research Online are protected by copyright, with all rights reserved unless indicated otherwise. They may be downloaded and/or printed for private study, or other acts as permitted by national copyright laws. The publisher or other rights holders may allow further reproduction and re-use of the full text version. This is indicated by the licence information on the White Rose Research Online record for the item.

Takedown

If you consider content in White Rose Research Online to be in breach of UK law, please notify us by emailing eprints@whiterose.ac.uk including the URL of the record and the reason for the withdrawal request.

Field observations of canopy flows over complex terrain

Eleanor R. Grant · Andrew N. Ross · Barry A.

Gardiner · Stephen D. Mobbs

the date of receipt and acceptance should be inserted later

Abstract The investigation of airflow over and within forests in complex terrain has been, until recently, limited to a handful of modelling and laboratory studies. Here, we present an observational dataset of airflow measurements inside and above a forest

E. R. Grant

Institute for Climate and Atmospheric Science, School of Earth and Environment, Univ. of Leeds, Leeds, UK. Present address: British Antarctic Survey, High Cross, Madingley Road, Cambridge, CB3 0ET, UK

A. N. Ross

Institute for Climate and Atmospheric Science, School of Earth and Environment, Univ. of Leeds, Leeds, LS2 9JT, UK. E-mail: A.N.Ross@leeds.ac.uk

B. A. Gardiner

Forest Research, Northern Research Station, Roslin, Midlothian EH25 9SY, Scotland. Present address: INRA, UMR 1391 ISPA, 33140 Villenave D'Ornon and Bordeaux Sciences Agro, UMR 1391 ISPA, 33170 Gradignan, France.

S. D. Mobbs

National Centre for Atmospheric Science and School of Earth and Environment, Univ. of Leeds, Leeds, LS2 9JT, UK.

9 situated on a ridge on the Isle of Arran, Scotland. The spatial coverage of the obser-
10 vations all the way across the ridge makes this a unique dataset. Two case studies of
11 across-ridge flow under near-neutral conditions are presented and compared with re-
12 cent idealized two-dimensional modelling studies. Changes in the canopy profiles of
13 both mean wind and turbulent quantities across the ridge are broadly consistent with
14 these idealized studies. Flow separation over the lee slope is seen as a ubiquitous
15 feature of the flow. The three-dimensional nature of the terrain and the heteroge-
16 neous forest canopy does however lead to significant variations in the flow separation
17 across the ridge, particularly over the less steep western slope. Furthermore, strong
18 directional shear with height in regions of flow separation has a significant impact on
19 the Reynolds stress terms and other turbulent statistics. Also observed is a decrease
20 in the variability of the wind speed over the summit and lee slope, which has not
21 been seen in previous studies. This dataset should provide a valuable resource for
22 validating models of canopy flow over real, complex terrain.

23 **Keywords** Boundary layer, Complex terrain, Flow separation, Forest canopy, Hills

24 **1 Introduction**

25 In recent years there has been a growing interest in the interaction of airflow within
26 and above forest canopies, particularly over complex terrain. This has been motivated
27 by a number of factors. For example, the uptake of carbon dioxide by forests is an
28 important and uncertain part of the carbon cycle. There has been a large worldwide in-
29 vestment in continuous measurements of the surface-atmosphere exchange of carbon
30 dioxide (Baldocchi et al., 2001) but interpretation of these measurements requires

31 a thorough understanding of canopy flows over complex terrain (Finnigan, 2008;
32 Belcher et al., 2008; Ross, 2011). Wind damage in hilly terrain is a serious threat
33 to managed forests (Quine and Gardiner, 2007; Gardiner et al., 2013) and reduces the
34 yield of recoverable timber, increases the cost of harvesting, decreases the landscape
35 quality and harms established wildlife habitats (Gardiner et al., 2010; Hanewinkel
36 et al., 2013). There is, to date, little theoretical framework for describing and under-
37 standing the turbulence structure within canopies on complex terrain, and yet this is
38 crucial for predicting wind damage to forests. Hills and mountains exert an impor-
39 tant drag on the atmosphere and this requires the correct parametrization in global
40 weather and climate models (Webster et al., 2003) but the presence of a forest canopy
41 can modify this drag (Ross and Vosper, 2005). Lastly, the large worldwide investment
42 in wind energy has wind turbines sited in forested areas of mixed topography. It is
43 therefore essential that the yield of these turbines is quantitatively understood (Ayotte
44 et al., 2001).

45 Airflow through forest canopies has been extensively studied for the last six
46 decades, but the majority of these studies have been restricted to idealized condi-
47 tions, i.e. homogeneous canopy, flat terrain, neutral to slightly unstable conditions
48 (see e.g. Kaimal and Finnigan, 1994; Finnigan, 2000). Most real forests are not ho-
49 mogeneous and are rarely on completely flat sites and so there is a fundamental need
50 to increase our understanding of these heterogeneous canopy flows. While there is
51 a considerable body of literature on flows over rough hills (Kaimal and Finnigan,
52 1994; Belcher and Hunt, 1998), it is only relatively recently that much attention has
53 been paid to canopy covered hills. This, to a large part, follows from the theoretical

54 work of Finnigan and Belcher (2004). In addition increasing attention has been paid
55 to heterogeneous canopy cover over the last 10 years, but again this has been largely
56 focused on sharp forest edge transitions (e.g. Irvine et al., 1997; Morse et al., 2002;
57 Dupont and Brunet, 2008; Romniger and Nepf, 2011).

58 Over the last twenty years there have only been a handful of observational stud-
59 ies of flow over forested complex terrain, the majority of which have been lim-
60 ited to wind-tunnel experiments, including Ruck and Adams (1991) and Neff and
61 Meroney (1998). Both studies investigated flow over modelled ridges covered with
62 plant canopies of differing heights. The wind-tunnel study of Finnigan and Brunet
63 (1995) conducted on a ridge covered with a tall canopy provided more comprehen-
64 sive measurements, showing that the inflection point at the top of the canopy profile
65 is heavily influenced by the presence of the hill. On the windward slope the inflection
66 point was observed to disappear while on the crest of the hill the strength of the in-
67 flection point was substantially greater. More recently a series of flume investigations
68 (Poggi and Katul, 2007a,b) explored the role of the hill-induced pressure perturbation
69 and advection on the flow velocity. Field experiments that have measured the airflow
70 at complex forested sites (e.g. Bradley, 1980; Zeri et al., 2010) have tended to make
71 measurements at a single tower and hence do not quantify the spatial variations in
72 flow across the terrain.

73 In addition to these observations there are a number of theoretical and modelling
74 studies, almost all of which make use of idealized terrain and a homogeneous, uni-
75 form canopy. Finnigan and Belcher (2004) extended the existing theory of Hunt et al.
76 (1988) for flow over rough hills and developed an analytical model for flow over

77 canopy covered hills. This model restricts itself to a shallow hill with a dense canopy
78 (all the momentum is absorbed by drag on the foliage) but it has clearly defined
79 the important parameters of the problem and offers a theoretical framework with
80 which to understand the earlier wind-tunnel results. Brown et al. (2001) and Allen
81 and Brown (2002) conducted large-eddy simulations (LES) and mixing length sim-
82 ulations of wind-tunnel observations using both a roughness length parametrization
83 and a canopy model. The canopy simulations modelled the observations with better
84 accuracy, showing reduced acceleration over the hill and an increase in the drag. Ross
85 and Vosper (2005) conducted a series of numerical simulations comparing the use
86 of an explicit canopy model with a roughness length parametrization. Results from
87 both roughness length and canopy simulations are compared to the observational data
88 of Finnigan and Brunet (1995), demonstrating the benefits of using a canopy model
89 over a roughness length parametrization. In the last few years three more notable LES
90 models have been developed. Dupont et al. (2008) analyze and validate results from a
91 nested LES using the wind-tunnel results of Finnigan and Brunet (1995); Ross (2008)
92 conducted LES of the flow over a series of small forested ridges; and Patton and Katul
93 (2009) used LES to explore the impact of vegetation density on the flow interactions
94 above and within vegetation on a series of gentle ridges. Other modelling studies have
95 looked at the impact of these canopy flows on tracer transport (Ross, 2011) and have
96 begun to explore the potential impact of non-homogeneous canopies over hills (Ross
97 and Baker, 2013). To date all of these theoretical and modelling studies have focused
98 on simple idealized terrain and, with the exception of Ross and Baker (2013), also
99 assume a uniform homogeneous canopy.

100 Thanks to the combined efforts of these studies we are now able to identify and
101 explain the key features of canopy flows over complex terrain, at least for a uniform
102 homogeneous canopy. However, there remain few studies over more complex and
103 realistic terrain with heterogeneous canopy cover. As has been pointed out (e.g. Poggi
104 and Katul, 2007a; Belcher et al., 2008), further progress has been restricted due to
105 a lack of the field measurements necessary to validate model developments. This
106 paper presents a unique observational dataset of airflow measurements from within
107 and above a forest situated on a ridge and compares the results to recent idealized
108 theoretical studies. It is the first dataset of its kind and should help to progress our
109 understanding of this subject. Section 2 gives an overview of the field experiment
110 and the data collected. Section 3 presents results from two particular case studies of
111 flow across the ridge under near-neutral conditions, concentrating on the mean flow
112 and the occurrence of flow separation. Section 4 provides details of profiles of various
113 turbulence statistics from the towers, while Sect. 5 discusses the results from this real,
114 complex and heterogeneous field site in the context of previous idealized models of
115 neutral flow over two-dimensional ridges covered with a uniform canopy. Results are
116 also compared with previous observations within and above flat, homogeneous forest
117 canopies in order to highlight the impact of the complex terrain on flow turbulence
118 characteristics. Finally Sect. 6 draws some conclusions.

119 **2 Overview of the field measurements**

120 The field measurements were made on a forested ridge, Leac Gharbh ($55^{\circ}40.2'N$,
121 $5^{\circ}33.6'W$), located on the north-east coast of the Isle of Arran, 22 km off the south-

122 west coast of the Scottish mainland. The island has previously been used for field
123 measurements of boundary-layer flow and flow separation over unforested hills (Vosper
124 et al., 2002). Typical hill heights at the northern end of Arran are between 400 m and
125 800 m with the island's highest hill, Goat Fell (874 m), lying 6 km to the south-
126 west of the field site. Leac Gharbh itself varies in height from approximately 160 m
127 at the south-east to 260 m at the north-west and is 1.5 km in length (Fig. 1). The
128 north-eastern slope of Leac Gharbh is steeper than the south-western slope (average
129 values of H/L are 0.36 and 0.24 respectively where H is the ridge height and L is
130 the half width of the hill) but the terrain on both slopes is inconsistent and there are
131 areas that are both significantly shallower and significantly steeper than these val-
132 ues. However, on average, both slopes are well above the typical values of 0.05 – 0.1
133 required for flow separation in a canopy (Ross and Vosper, 2005; Poggi and Katul,
134 2007b). The summit of the ridge is approximately 250 m wide. The ridge is forested
135 primarily with a dense (1600 trees per hectare) Sitka spruce (*Picea sitchensis* Bong.
136 Carr.) plantation with an average tree height of $h = 17.5$ m. There are also patches
137 of western hemlock (*Tsuga heterophylla*) and silver birch (*Betula pendula*) mixed in
138 with the Sitka spruce, particularly on the north-east slope. To the southern end of the
139 ridge there are also hybrid larch (*Larix x marschlinsii* (Syn. *L. x eurolepis*)) of a simi-
140 lar height to the Sitka spruce. Further north along the ridge and beyond the forest the
141 land cover is rough moorland. A detailed analysis of the forest canopy was conducted
142 by the Forestry Commission, with the survey splitting the site into 23×0.01 ha plots
143 (Fig. 1), and for each plot the number, species and diameter at breast height (1.3 m
144 above ground) of each tree was recorded. The height of the tree with the greatest di-

145 ameter was also recorded. As the aerial photograph in Fig. 1 shows the density of the
146 canopy varies significantly over the field site and there are several large clearings, the
147 largest of which is $5h$ across.

148 Measurements were made continually from 13 March to 14 May 2007. Three ver-
149 tical profile towers (T1, T2, T3) were located across the ridge, and were supplemented
150 with a network of 12 automatic weather stations (AWS) giving measurements near the
151 surface (2 m above the ground). The AWS are labelled ARA through to ARQ and the
152 location of each site is shown in Fig. 1. Four three-dimensional sonic anemometers
153 sampling at 10Hz were mounted on each tower along with six thermistor temper-
154 ature sensors and six cup anemometers at various heights between 2 m and 23 m.
155 The sonic anemometers were logged using a Moxa UC-7420 low power computer
156 at each tower running custom logging software. One-minute average values from the
157 cup anemometers and thermistors were logged with a Campbell CR1000 data logger
158 at each tower. Each AWS measured wind speed and wind direction at 2 m (with a
159 wind cup and vane), temperature (with a thermistor and with a Sensiron SHT1x digi-
160 tal sensor) and pressure. The AWS logged data every 3 s using a custom made lower
161 power data logger. Table 1 in Appendix 1 provides a detailed overview of the instru-
162 ments used. All instrumentation was deployed within an area of less than 2 km^2 . The
163 vertical profile towers were constructed in a transect over the ridge (henceforth, the
164 canopy transect), with Fig. 1 showing the location of each tower and AWS. The ma-
165 jority of the AWS were erected in the same transect as the profile towers to provide as
166 much information as possible over this specific area. A second, smaller transect was
167 constructed well outside the forest ridge canopy using three AWS (henceforth the

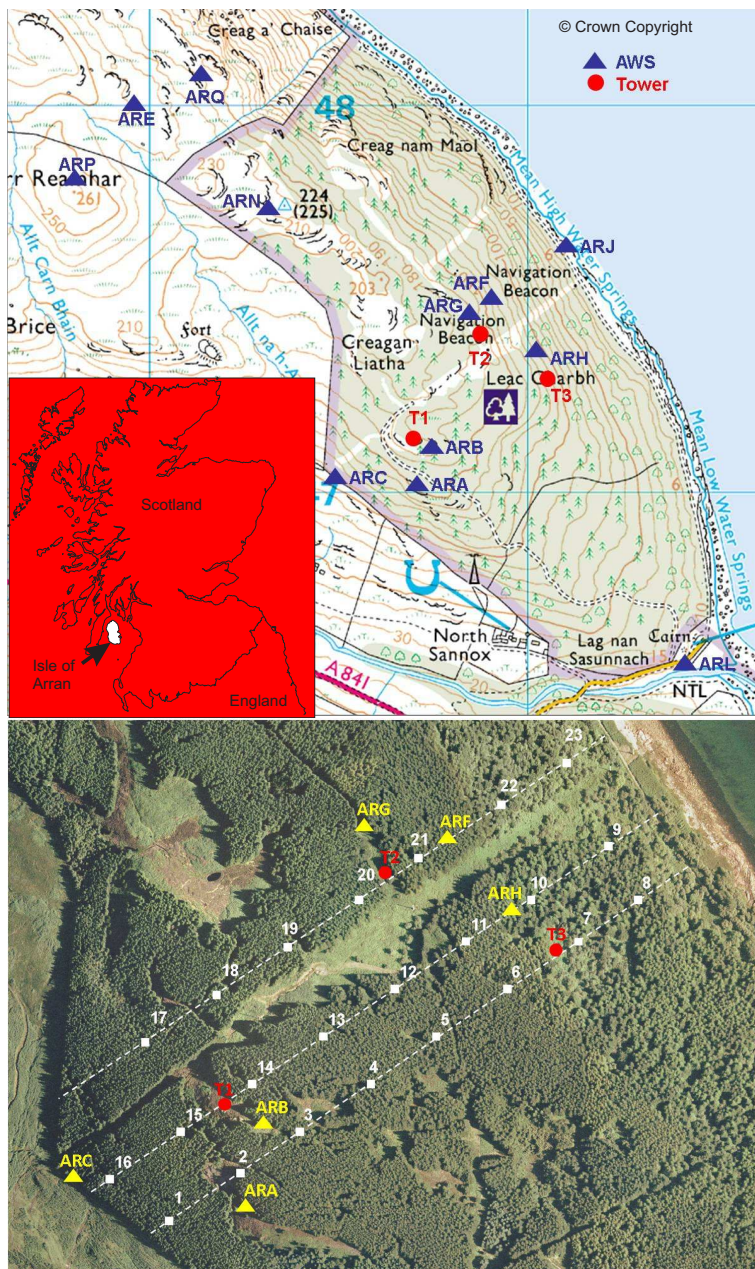


Fig. 1 Top: 1:25000 Ordnance Survey map of the field site with instrumentation sites marked. Red circles indicate the vertical profile towers (T1, T2, T3) and blue triangles indicate automatic weather stations (AWS). Inset is a map of Scotland highlighting the location of the Isle of Arran. The 1:25000 map is © Crown Copyright / database right 2010. An Ordnance Survey / EDINA supplied service. Outline map of Scotland is reproduced from Ordnance Survey map data by permission of Ordnance Survey, © Crown copyright 2013. Bottom: aerial photograph of the field site canopy showing the 23 canopy survey plots (white squares), the tower sites (red circles) and the AWS (yellow triangles). The white squares of the survey plots are to scale.

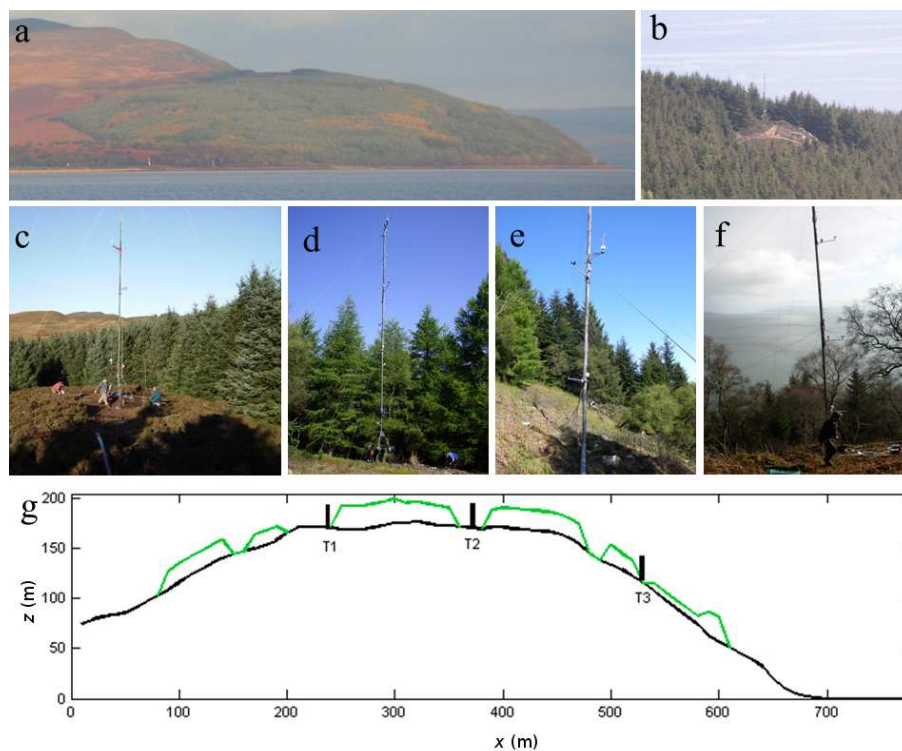


Fig. 2 Photographs from the field site showing (a) Leac Gharbh, taken from the sea looking north-west. (b) Taken from AWS ARP, looking south-east, down onto T1. T1 is elevated slightly from its surroundings and is in a clearing that is approximately three canopy heights wide and five canopy heights long. (c) T1 looking north-west, showing the dense canopy to the north and east of the tower and the large clearing to the west. (d) The site at T2 looking north-east, showing the larch canopy. To the west the canopy is Sitka spruce. These two canopies are divided by a small pathway to the north-west which leads to AWS ARG. (e) T3 looking north-west, showing the dense spruce plantation upslope. (f) T3 looking east. This picture illustrates the steepness of the terrain downslope from T3. It also shows how some of the canopy (of mainly birch) directly downslope of the tower does not reach the same level as the bottom sonic anemometer, which is just visible to the right of the tower above the second cup anemometer. (g) Schematic cross-section profile (west to east) of Leac Gharbh with tower locations shown and canopy marked in green.

168 northern transect), and at each site a differential GPS survey was conducted to calcu-
169 late altitude accurately. Tables 2 and 3 in Appendix 1 summarize the main features of
170 each instrument site.

171 For the results presented here the 3-s data from the AWS were averaged. The
172 mean wind speed is the 15-min average of the instantaneous wind speeds and the
173 mean wind direction was determined as the direction of the averaged instantaneous
174 wind vectors over the same period. The wind speeds presented here from the sonic
175 anemometers are 15-min averages of the instantaneous wind speeds (for direct com-
176 parison with the cup anemometers). Wind directions are again the direction of the
177 mean wind vector. For calculating momentum fluxes each 15-min period of data was
178 rotated into streamwise coordinates using a double rotation (see e.g. Lee et al., 2004).
179 The presented fluxes are therefore in streamwise coordinates, with u being in the di-
180 rection of the 15-min averaged mean wind. The flux data were quality controlled
181 using the stationarity test of Foken and Wichura (1996) with each 15-min period
182 subdivided into five, and a 30% threshold for the differences to be classified as non-
183 stationary. At the more exposed sites this resulted in less than 1% of the data being
184 rejected, but at some of the more sheltered in-canopy sites up to 10% of the data was
185 rejected. Following data quality control, continuous operation for 44 days between 1
186 April and 14 May 2007 provided 4224 15-min mean measurements from the major-
187 ity of the AWS and vertical profile towers. Quality controlled data between 13 March
188 and 31 March 2007 are also available but these data are incomplete. The following
189 analysis only uses data from 1 April until 14 May 2007, after bud burst on the trees.

190 This minimizes the impact of changing leaf cover on the canopy drag, and hence the
 191 flow patterns in the patches of deciduous trees (mainly birch and larch).

192 The field campaign was dominated by anticyclonic conditions with anticyclones
 193 located over Arran for 24 of the 44 days. These anticyclonic periods were associated
 194 with low wind speeds from the north to east and a well-defined diurnal cycle was
 195 established in the potential temperature time series. These periods were interspersed
 196 with two large cyclonic systems and a series of fronts. The cyclonic systems coin-
 197 cided with high wind speed south-westerlies and a breakdown of the diurnal cycle
 198 established during the anticyclonic periods.

199 In order to compare the field observations with theory developed from 2-D, neu-
 200 tral flow over forested ridges we concentrate on periods when the synoptic flow is
 201 across the ridge. Cross-ridge flows were defined when the angle of the synoptic flow,
 202 α , is $50^\circ < \alpha < 90^\circ$ (henceforth, north-easterlies) and $240^\circ < \alpha < 260^\circ$ (henceforth,
 203 south-westerlies). The south-westerly cases based on wind direction at AWS ARP
 204 amounted to 50 h of data. North-easterlies were determined when both AWS ARP
 205 and the top sonic anemometer on T3 recorded wind directions between $\alpha = 50^\circ$ and
 206 $\alpha = 90^\circ$. This amounted to 15 h of data. Data from both AWS ARP and tower T3 are
 207 used to identify north-easterlies and so rule out any cases of south-westerly flow sep-
 208 aration. The 40° window for north-easterlies is used to allow a large enough sample.

209 To restrict the comparison to near-neutral conditions the data are also filter based
 210 on h/L calculated at the top of tower T1 (the most exposed site), where L is the
 211 Obukhov length given by

$$L = \frac{(-\overline{u'w'})^{3/2}\theta}{\kappa g \overline{w'T'}}, \quad (1)$$

212 where $\overline{u'w'}$ is the momentum flux, $\overline{w'T'}$ is the kinematic heat flux, θ is the absolute
213 potential air temperature (K), $g = 9.81 \text{ ms}^{-2}$ is the acceleration due to gravity, and
214 $\kappa = 0.4$ is the von Karman constant. Following Dupont and Patton (2012), we restrict
215 the data to cases where $-0.01 \leq h/L < 0.02$ (near neutral) and $0.02 \leq z/L < 0.6$
216 (transition to stable). In their comparison of data over a flat orchard site during the
217 CHATS experiment Dupont and Patton (2012) observed similar features of the flow
218 structure in these two regimes. Limiting to near-neutral cases only would result in a
219 rather small sample size. These regimes occurred mostly during windy and / or cloudy
220 periods with low radiative forcing, or around the evening / morning transitions when
221 the sensible heat flux is small. The south-westerly cases in particular are associated
222 with stronger winds and a weak diurnal cycle of temperature. The north-easterly cases
223 associated with high pressure are generally weaker winds and a stronger diurnal cycle
224 so the selected cases occur around the evening and morning transitions.

225 **3 Flow structure and flow separation**

226 Figure 3a-f shows 15-min averaged tower data for all times when the synoptic flow
227 was south-westerly with Fig. 3a-c showing velocity profiles for each tower. The
228 coloured circles show data from the sonic anemometers (coloured according to wind
229 direction) and the black crosses are data from the cup anemometers. The interquartile
230 ranges (25th – 75th percentile) of the 15-min mean wind-speed data for all south-
231 westerly periods are shown as horizontal bars. Figure 3d-f shows vertical momentum-
232 flux profiles for each tower, where again the sonic anemometer data are coloured ac-
233 cording to wind direction and interquartile ranges are shown. Figure 4 shows wind

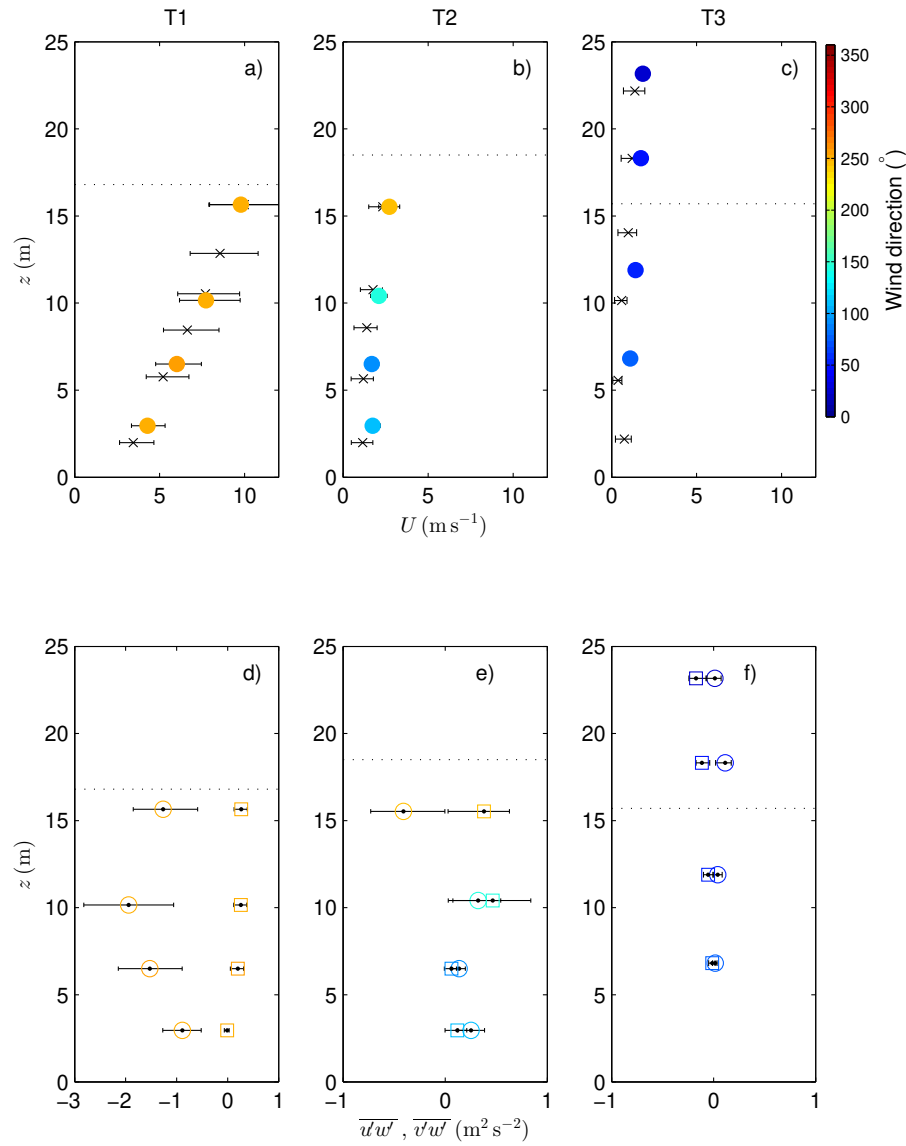


Fig. 3 (a-c): Wind-speed profiles for each tower during south-westerly flow. Cup anemometer data are indicated by black crosses with sonic anemometer data indicated by coloured circles, coloured according to mean wind direction. The error bars show the interquartile range of the 15-min mean wind-speed data. Canopy height is indicated by a dashed line. (d-f): Vertical momentum-flux profiles $\overline{u'w'}$ (circles) and $\overline{v'w'}$ (squares) for each tower during south-westerly flow, data coloured according to mean wind direction. Interquartile ranges of the 15-min mean momentum fluxes are shown.

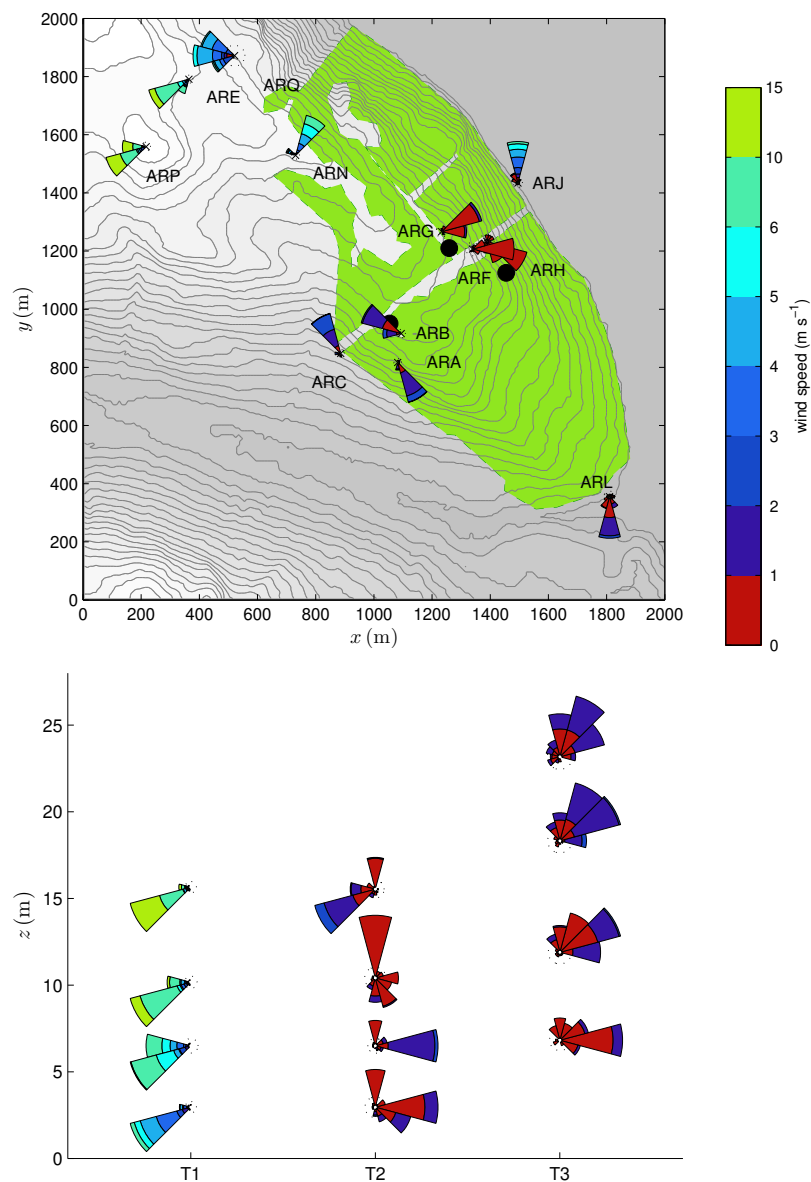


Fig. 4 15-min averaged wind data from the AWS and sonic anemometers for all times when the synoptic flow was south-westerly showing (top): frequency distribution wind roses for wind direction, coloured according to wind speed in m s^{-1} for each AWS. Dashed radius indicates a frequency of 5%. Wind roses plotted on a contour map of field site, terrain contours plotted at 10-m intervals, shaded green marks the forest, black dots mark tower locations. (Bottom): Frequency distribution plots for wind direction, coloured according to wind speed in m s^{-1} for each tower.

234 roses of 15-min averaged wind data for the same period for the AWS (top panel) and
235 towers (bottom panel). The AWS cup anemometers are subject to a 0.78 m s^{-1} stalling
236 threshold, and so data $< 1 \text{ m s}^{-1}$ (coloured red) should be treated with caution. The
237 sonic anemometers do not have a stalling threshold so low wind-speed data from the
238 towers can be treated normally. Similar plots for cases when the synoptic flow was
239 north-easterly are shown in Figs. 5 and 6.

240 For south-westerly flow (Figs. 3a-c and 4) the observations show strong evidence
241 of flow separation, with the flow at tower T3 on the lee slope being predominantly
242 north-easterly or easterly. Tower T2 on the top of the ridge appears to be close to the
243 separation point with reversed, easterly flow deep within the canopy, but with south-
244 westerly flow near canopy top. The AWS wind data in Fig. 4 support this conclusion,
245 with flow from the north-east to south-east over the lee slope (AWS ARG, ARF and
246 ARH), and also at the AWS near the summit (ARN). This suggests a large region
247 of flow separation covering most of the lee slope where there is significant forest
248 cover. Note that within the canopy over the lee slope wind speeds are very low, almost
249 exclusively in $< 1 \text{ m s}^{-1}$. Flow separation along the ridge crest is less apparent outside
250 the forested region, with AWS ARQ still showing broadly westerly flow, although
251 the flow appears to be more north-westerly than south-westerly perhaps indicating
252 the commencement of some flow separation. The AWS ARN site, which is on clear
253 ground, but with trees to both the south-west and north-east, shows a reversal of
254 winds. The east slope of the ridge is sufficiently steep that flow separation might
255 occur even in the absence of the canopy, however it seems unlikely that this would
256 happen at AWS ARN. Interestingly there is considerable variability in wind direction

257 over the upwind slope as well, with AWS ARA, ARB and ARC exhibiting either
258 north-westerly or south-easterly flow.

259 In south-westerly flow the stronger winds at tower T1 lead to enhanced shear and
260 a larger along-stream momentum flux, $\overline{u'w'}$ compared to the other two towers. The
261 relatively exposed site implies that the wind shear exists right down to the surface,
262 and that the flow cannot be considered as a pure canopy flow. The uniform wind
263 direction means the cross-stream momentum flux, $\overline{v'w'}$ is much smaller. The large
264 negative values of $\overline{u'w'}$ at the top of tower T2 (Fig. 3 e) indicate a downward flux
265 of momentum as faster moving air above the canopy is drawn down into the canopy.
266 However, further down in the canopy $\overline{u'w'}$ is positive indicating that momentum in
267 the along-flow direction in local streamline coordinates is transported upwards. This
268 is somewhat counter-intuitive at first glance, but can be explained by the directional
269 shear with height caused by the region of flow separation. This results in du/dz in
270 streamwise coordinates being small or negative throughout much of the canopy, al-
271 though the wind speed increases with height. Alongside the positive $\overline{u'w'}$, larger val-
272 ues of $\overline{v'w'}$, similar in magnitude to $\overline{u'w'}$, are observed, which is again consistent with
273 directional shear being important. At tower T3 the region of separated flow appears
274 to extend above the tower and inside the separation region winds are very light with
275 little variation in wind speed or direction with height, consistent with the small and
276 almost constant momentum flux. Since the change in wind speed is very small, the
277 directional shear that is present gives rise to the small positive $\overline{u'w'}$ values at T3.

278 For north-easterly flow (Figs. 5(a)-(c) and 6) wind speeds are lower than for the
279 south-westerly cases. Consequently the flow patterns over the ridge are less defined,

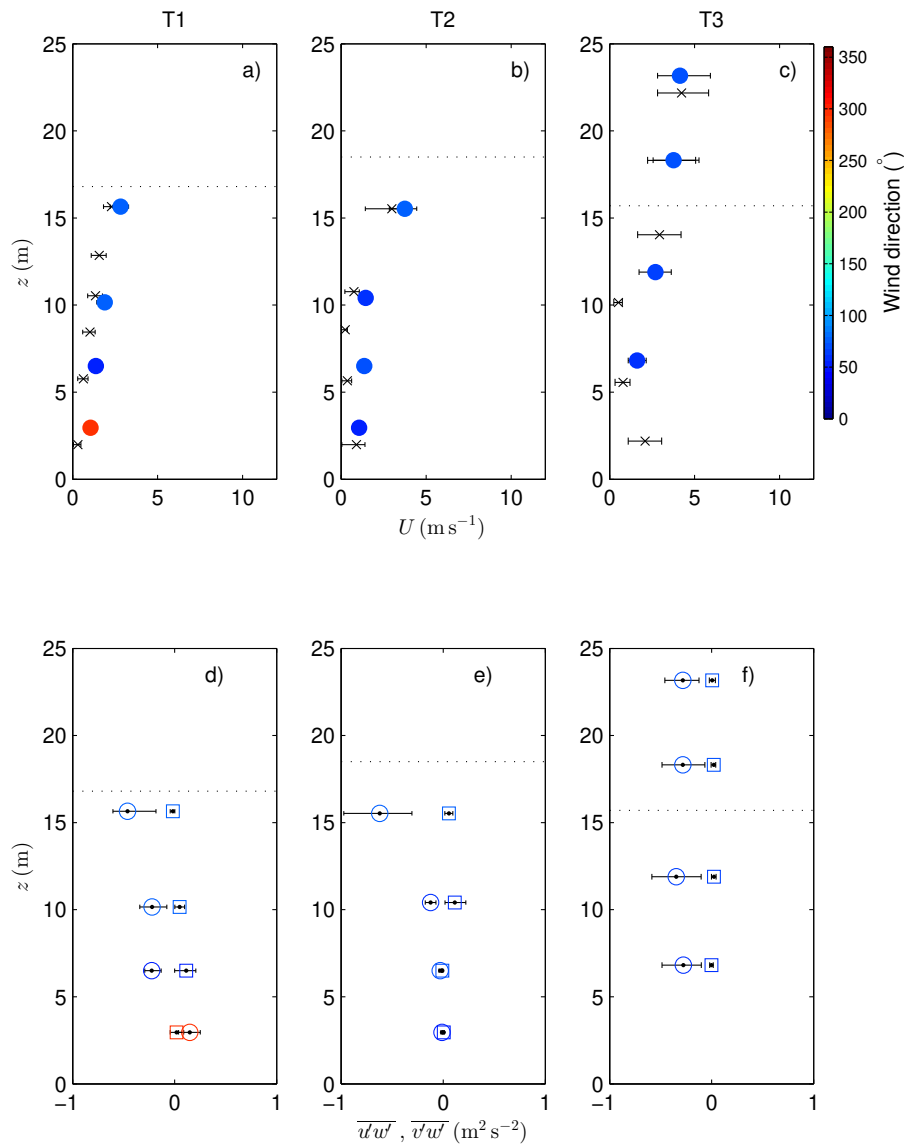


Fig. 5 As Fig. 3, but for north-easterly cases.

280 with much of the AWS data showing windspeeds below the 1 m s^{-1} threshold. The
 281 upwind profile at T3 shows much stronger winds than in south-westerly flow, even
 282 though synoptic winds are lighter. The profile above the canopy also appears closer

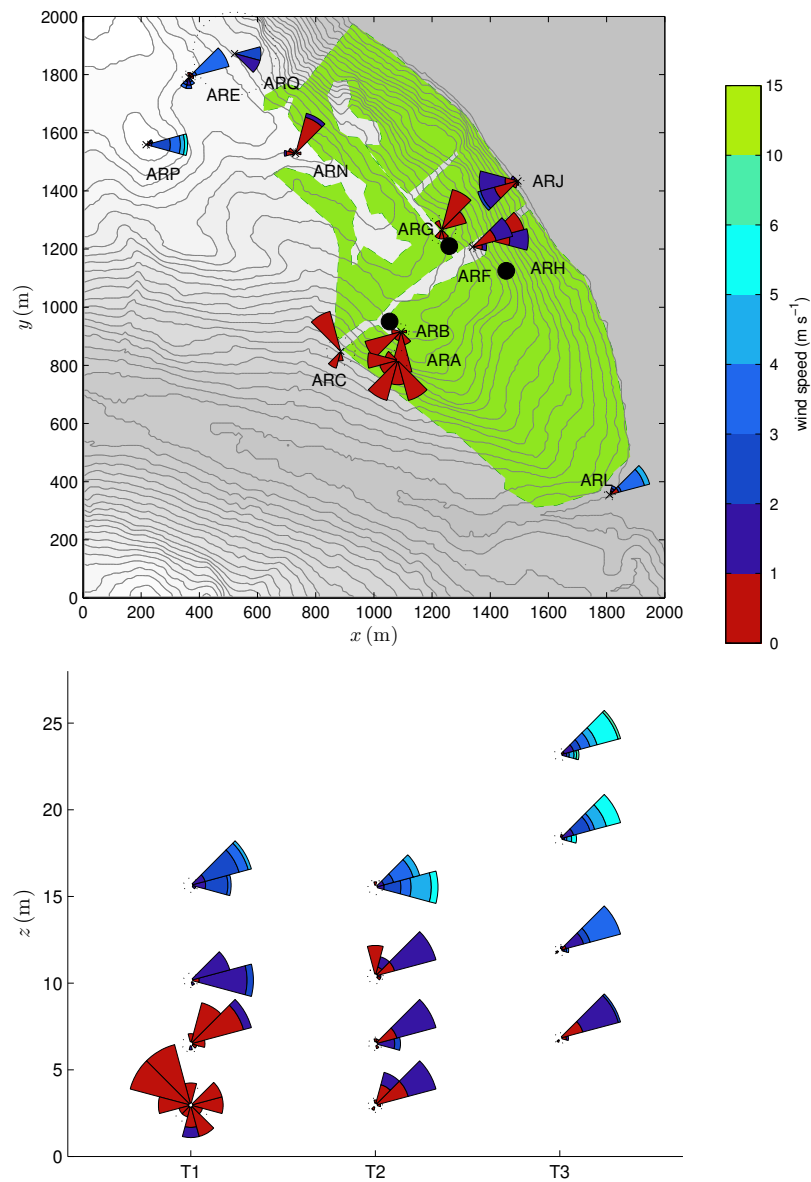


Fig. 6 As Fig. 4, but for north-easterly cases.

283 to logarithmic in character than the south-westerly flow case where tower T3 was in
 284 the separation region; this is consistent with the nearly constant profile of $\overline{u'w'}$ and
 285 negligible $\overline{v'w'}$. For this north-easterly case there is less evidence of flow separation

286 from the tower data over the summit and in the lee. The flow at tower T2 remains
287 north-easterly, and at tower T1 the flow is also north-easterly except at the lowest
288 measurement height. At this height (2.96m) the flow is very variable in direction,
289 but having a more westerly component. The AWS data in Fig. 6 do however provide
290 further evidence of flow separation, with flow at sites on the windward slope being
291 predominantly north-easterly, while over the lee slope the winds are again very light
292 and variable with flow broadly south-westerly. The weaker and shallower flow separation
293 seen in this case is likely to be explained by the less steep lee slope and also
294 the fact that tower T1 is closer to the summit of the ridge than is tower T3. As in
295 the south-westerly case there is no strong evidence of flow separation on the transect
296 outside the forest canopy. The AWS ARJ site, at the upwind foot of the ridge, does
297 show a reversal in the flow, with consistently westerly or south-westerly winds. This
298 is a recurring feature of the easterly flow over this ridge and is attributed to the blocking
299 of the low-level flow by the steeply rising land and the forest edge. At tower T1,
300 despite the tower being mostly outside the separation region, the wind speeds decay
301 relatively slowly with height in the canopy, and as a result the momentum flux values
302 also only decay slowly with height (Fig. 5 a). At the lowest point on tower T3 there
303 is evidence of a sub-canopy jet near the ground due to the lower canopy density in
304 the trunk space compared to higher up in the canopy. This feature is present at tower
305 T3 in the south-westerly case as well, but is less distinct due to the generally weaker
306 flow in the separation region. For north-easterly flow there is also some evidence of
307 a sub-canopy jet at tower T2, which is not present in the south-westerly cases. This
308 is due to differences in the canopy cover, with the canopy to the west of tower T2

309 being much denser Sitka spruce, with the trees to the east consisting of a mix of Sitka
310 spruce and hybrid larch with a much more pronounced trunk space.

311 One further noticeable feature of the wind profiles in Figs. 3 a-c is the much
312 larger variability in 15-min mean wind speeds on the upwind slope, evident from
313 the wider interquartile spread. One would expect a larger range of wind speeds at
314 tower T1 because the mean wind speed is higher. One normalized measure of the
315 variability is the interquartile range divided by the mean wind speed (i.e. the width
316 of the error bars divided by the mean values in the figure). At tower T1 this gives
317 values of 0.78–0.82, but in comparison, at towers T2 and T3 values are smaller, in
318 the range of 0.44–0.51 and 0.39–0.57 respectively. Wind speeds are often assumed to
319 follow a Weibull distribution (e.g. Justus et al., 1976, and many subsequent studies),
320 with a shape parameter k close to 2. Assuming this distribution, then the normalized
321 interquartile range can be calculated as approximately 0.72. This suggests that winds
322 on the upwind slope are slightly more variable than might be expected, while those
323 over the summit and in the lee demonstrate significantly less variability. The north-
324 easterly cases show a similar pattern of variability in wind speeds as occurs in the
325 south-westerly cases, with much higher variability at the upwind tower T3 (0.67–
326 1.08) compared to tower T2 at the summit (0.36–0.58) and T1 on the lee slope (0.35–
327 0.43). This therefore seems to be a robust feature of these canopy flows.

328 **4 Profiles of turbulence statistics**

329 Here, we present profiles of various turbulence statistics calculated from the sonic
330 anemometer data at the three tower sites over the hill. Figure 7a-c shows profiles of

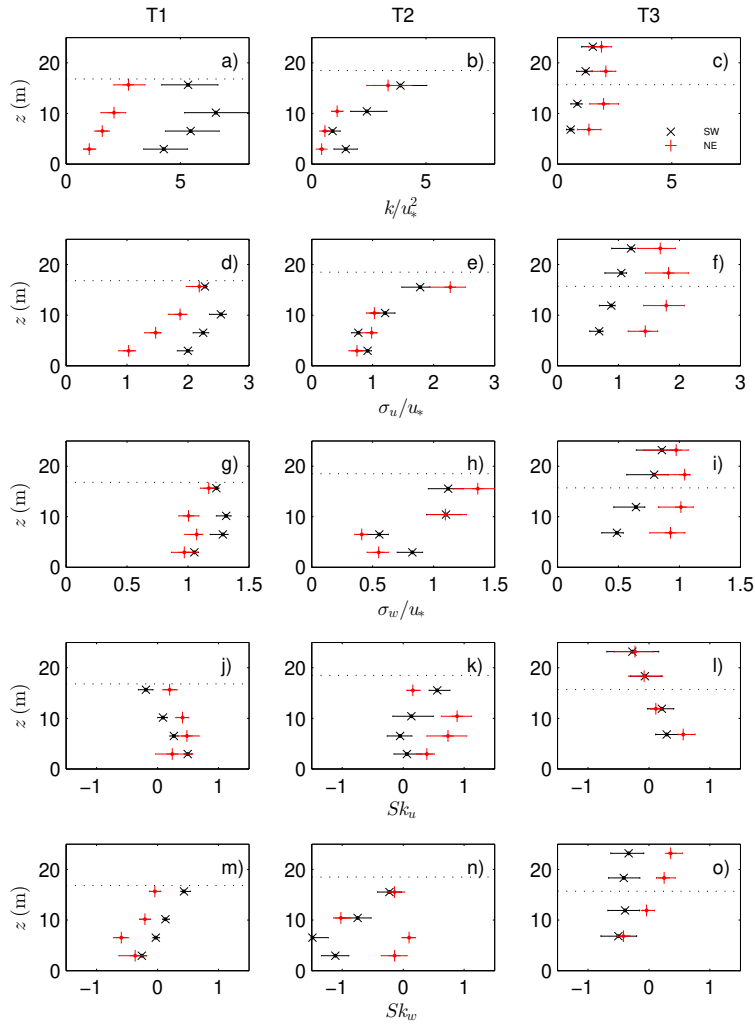


Fig. 7 Profiles of (a-c) turbulent kinetic energy k normalized by the friction velocity u_* squared, (d-f) horizontal variance normalized by the friction velocity, (g-i) vertical velocity variance normalized by the friction velocity, (j-l) horizontal velocity skewness Sk_u and (m-o) vertical velocity skewness Sk_w . Profiles are plotted for both south-westerly (\times) and north-easterly ($+$) cases at each tower. For each plot the error bars show the interquartile range of the 15-min averaged data.

331 turbulent kinetic energy, k , normalized by the friction velocity squared ($u_*^2 = \overline{|u'w'|}$)
332 calculated at the top of tower T1. This is used as a reference since it is relatively
333 exposed and gives an indication of the overall flow at a given time. Similarly Fig. 7
334 presents profiles of both (d-f) horizontal velocity variance (σ_u) and (g-i) vertical ve-
335 locity variance (σ_w) normalized by u_* at the top of tower T1. Using a single value
336 of u_* allows the relative magnitude of k , σ_u and σ_w at the different towers to be as-
337 sessed. It is immediately obvious that tower T1 exhibits the highest levels of turbulent
338 kinetic energy and velocity variances, particularly in south-westerly flows. Given the
339 relatively exposed location of tower T1 this is perhaps not surprising, since in a north-
340 easterly flow, where tower T1 is slightly more sheltered, turbulence levels are lower.
341 At tower T3 turbulence levels are generally lower than at tower T1, possibly due to
342 the less exposed site, although again there is evidence of higher turbulent kinetic en-
343 ergy and velocity variance levels when the flow is from the north-east compared to
344 the south-west. It is interesting to note that increased variability in the normalized
345 15-min mean wind at the upwind tower (Figs. 3 and 5) corresponds to increased nor-
346 malized turbulence levels (the mean of the 15-min TKE values). At tower T2 near
347 the summit there is less difference in the magnitude of the turbulence levels between
348 the two wind directions, especially at the top of the tower. What is obvious is a more
349 rapid increase in k , σ_u and σ_w in the upper canopy compared to that at towers T1 and
350 T3, probably related to the increased wind shear due to changes in both wind speed
351 and direction with height. Profiles of the vertical velocity variance, σ_w/u_* , show typi-
352 cally smaller values than the corresponding horizontal velocity variances with values
353 at and above canopy top around $\sigma_u/u_* = 1.5 - 2.5$ and $\sigma_w/u_* = 1 - 1.5$.

Profiles of horizontal and vertical skewness are given in Fig. 7(j-o) where the
 skewness is given by $Sk_\chi = \overline{\chi^3} / (\overline{\chi^2})^{3/2}$ and χ is either the horizontal velocity com-
 ponent u or the vertical velocity component w . In contrast to the turbulent kinetic
 energy and intensity profiles, towers T1 and T3 show similar profiles of skewness in
 both upwind and downwind cases. For both towers the skewness is relatively small
 at and above canopy top, but increases deeper into the canopy, with $Sk_u \approx 0.5$ and
 $Sk_w \approx -0.5$ near the ground. In contrast, bigger variations in skewness are seen be-
 tween cases at tower T2. For south-westerly flow Sk_u remains small throughout the
 profile, with the largest values being near canopy top. In this case Sk_w is small at
 canopy top, but with large values of about -1 within the canopy. It is possible that
 this very different pattern of skewness is related to the strong directional shear seen
 at tower T2 for south-westerly cases where the tower is located close to the sepa-
 ration point of the flow. In contrast, for north-easterly flow the profiles of Sk_u are
 more typical, with small values at canopy top and larger values within the canopy.
 Sk_w however shows a peak at about 10m (below canopy top), with values deeper in
 the canopy dropping close to zero again. Large changes in wind direction with height
 are not present at tower T2 in the north-easterly cases, however $\overline{v'w'}$ is comparable
 to $\overline{u'w'}$ at this height suggesting that the flow is not representative of flow over an
 idealized homogeneous canopy.

373 5 Discussion

374 5.1 Comparison with idealized models of flow over a forested hill

375 From previous theoretical studies (e.g. Finnigan and Belcher, 2004), numerical sim-
376 ulations (e.g. Ross and Vosper, 2005) and laboratory experiments (such as Finnigan
377 and Brunet, 1995; Poggi and Katul, 2007b) we have an idealized conceptual picture
378 of flow over a two-dimensional forested ridge. The key features of this conceptual
379 picture are seen in the field observations presented here. The ridge has slopes > 0.1 ,
380 and so based on Ross and Vosper (2005) we might expect flow separation. This is
381 indeed observed, both at the towers and at the AWS. As would be expected flow sep-
382 aration appears to be stronger for south-westerly cases where the lee slope is steeper.
383 Unlike the simple two-dimensional model, flow is not simply reversed over the lee
384 slope, and there may be significant along-slope components to the flow in these flow
385 separation regions (e.g. at AWS ARA, ARB and ARC in Fig. 6). Both the three-
386 dimensional nature of the terrain and the heterogeneous nature of the canopy appear
387 to be important in determining the exact nature of the separated flow.

388 In previous idealized studies differences in the induced flow within and above the
389 canopy lead to changes in the shear layer at canopy top across the hill. Over the up-
390 wind slope the shear is reduced since there is relatively little acceleration of the flow
391 above the canopy, but there is induced upslope flow within the canopy. Near the sum-
392 mit the above-canopy flow accelerates to its maximum speed, while the in-canopy
393 flow decelerates, leading to an increase in the shear layer and a sharp inflection point
394 in the velocity profile. Over the lee slope the development of a region of flow sep-

395 aration leads to low wind speeds and reversed flow direction in the canopy. Again
396 we also see these features qualitatively in the field observations presented here (e.g.
397 Figs. 3 and 5). For the south-westerly case this is enhanced by the fact that tower T1
398 is at a relatively exposed site and so the flow is not a pure canopy flow. Near the sum-
399 mit at tower T2 we do see a large increase in the momentum flux and some evidence
400 of the inflection point in the velocity profile, however to really confirm this would
401 require observations further above the canopy. As might be expected, the reduced
402 shear over the upwind slope leads to a reduction in the generated turbulent mixing at
403 canopy top in this region, although the fact that there is a mean flow component into
404 the canopy implies that turbulence levels in the upper canopy can actually increase
405 due to vertical advection of more turbulent air from above. There is some evidence
406 of this at towers T1 (for south-westerly flow) and T3 (for north-easterly flow) in both
407 the momentum-flux profiles (Figs. 3 and 5) and the turbulent kinetic energy profiles
408 (Fig. 7).

409 For south-westerly flow the tower on the lee slope (T3) shows evidence of the
410 flow separation region extending well above the canopy top. Since this slope is signif-
411 icantly steeper than the critical slope for flow separation to extend above the canopy
412 found by Ross and Vosper (2005) this is not too surprising. It is interesting that we do
413 not see the same features at tower T1 for north-easterly flow, even though the western
414 slope is still relatively steep, although less steep than the eastern slope. The differ-
415 ences in the site may well play a role here. Tower T1 is more exposed with a relatively
416 large clearing to the west. The profiles of $\overline{u'w'}$ in Fig. 5 suggest there is significant
417 mixing of momentum down into the canopy, and this is supported by the wind speed

418 profile which shows little sign of a strong inflection point near canopy top. Miller
419 et al. (1991) and Belcher et al. (2003) have shown that, over flat ground, the mean
420 wind speed rapidly increases as the flow leaves the canopy in response to the removal
421 of the drag force associated with the canopy, and that there is a downward motion
422 into the clearing to conserve mass. With its location at a distance of approximately
423 h from the forest edge, tower T1 is very likely to be affected by these features in
424 north-easterly flow. As shown by Ross and Baker (2013) in their idealized modelling
425 study, the flow over complex terrain with heterogeneous canopy cover is driven by a
426 combination of canopy edge induced and terrain-induced pressure perturbations. Rel-
427 atively localized canopy-edge effects will dominate near to the canopy edge, while
428 elsewhere terrain effects will dominate. In their simulations Ross and Baker (2013)
429 observed that flow separation was primarily constrained to within the canopy over
430 moderate slopes, only extending a short distance beyond the edge of the canopy over
431 the lee slope. This is consistent with the shallow separation observed here at tower
432 T1.

433 The impact of forest edges and clearings can also be used to explain the south-
434 easterly winds recorded at AWS ARA during south-westerlies (Fig. 4). The theoret-
435 ical model of Belcher et al. (2003) predicts an adverse pressure gradient upwind of a
436 clearing to canopy transition, which acts to decelerate the flow as it approaches the
437 forest edge. In three dimensions this deceleration may lead to deflection of the flow
438 along the canopy edge (as seen at AWS ARA, ARB and ARC), or even to flow rever-
439 sal (e.g. AWS ARJ). Similar flow separation at the upwind edge of the canopy is seen
440 in the large-eddy simulations of Cassiani et al. (2008) over flat ground and also at the

441 upwind canopy edge on the upwind slope in the idealized two-dimensional numerical
442 simulations of Ross and Baker (2013).

443 5.2 Comparison of turbulence statistics with idealized models

444 The profiles of turbulent statistics presented in section 4 are broadly consistent with
445 previous observations over flat, homogeneous canopies, as summarized for example
446 by Raupach et al. (1996) who present data from a number of different experiments
447 over very different (but homogeneous) canopies. Few of the idealised studies over
448 hills (either experimental or numerical) include turbulent statistics, however there
449 are wind-tunnel observations presented in Finnigan and Brunet (1995). Dupont et al.
450 (2008) largely reproduced these observations in their large-eddy simulation, includ-
451 ing additional observations unpublished in the original paper of Finnigan and Brunet
452 (1995). Again these profiles over an idealised ridge are largely consistent with the
453 real field observations presented here. Below we highlight the key differences.

454 As in Finnigan and Brunet (1995) and Dupont et al. (2008), higher values of
455 σ_u/u_* and σ_w/u_* are observed in the lower canopy at the upwind tower (T1 for
456 south-westerly flow and T3 for north-easterly flow). This is likely to be due to the
457 mean flow into the canopy leading to advection of turbulence from the upper canopy,
458 and is in line with the observed increase in turbulent kinetic energy at these loca-
459 tions. Low values of σ_u/u_* and σ_w/u_* are observed above the canopy on tower T3
460 in south-westerly winds, probably because T3 is entirely within the separation region
461 and subject to weak winds and low shear even above the canopy. The only point on
462 tower T2 which seems to deviate from previous results over flat ground and from

463 the wind-tunnel data is the lowest instrument height in south-westerly winds, which
464 shows larger values of σ_w/u_* than expected (about 0.8), which are also significantly
465 larger than at the height above. At this lowest height slightly elevated values of k/u_*^2
466 are also observed, along with positive momentum fluxes, larger in magnitude than
467 at the height above. There is relatively little evidence of trunk space flow in these
468 conditions (thick Sitka spruce to the west of the tower), and so the increased tur-
469 bulence is probably related to the strong directional shear and is a feature of the
470 three-dimensional flow in this non-idealized situation.

471 In Finnigan and Brunet (1995) and Dupont et al. (2008) the skewness changes
472 relatively little over most of the hill, with small values of both Sk_u and Sk_v aloft and
473 Sk_u increasing to 1 to 1.5 in the canopy and Sk_w decreasing to -1 to -1.5 . These
474 are slightly higher in magnitude than many of the profiles presented in Raupach et al.
475 (1996) for canopies on flat ground and the values do not decrease with height lower
476 down in the canopy. This is probably a reflection of the modelled canopy in the wind
477 tunnel rather than the fact that the flow is over a ridge. Values are quite variable in
478 the wind-tunnel data over the summit and just downwind, but there does appear to
479 be peaks in both Sk_u and Sk_w near canopy top over the summit. In the recirculation
480 region in the wind tunnel Sk_u takes its largest positive values and Sk_w takes its largest
481 negative values. The variations in skewness across the hill seen in the field observa-
482 tions presented here are broadly consistent with those in Finnigan and Brunet (1995),
483 although the values of the skewnesses are less than those seen in the wind-tunnel
484 experiments. The key location where the skewness differs from the results over flat
485 ground presented in Raupach et al. (1996) is at tower T2 in south-westerly winds

486 where Sk_u is small throughout most of the canopy, only increasing towards canopy
487 top. In contrast Sk_w has large negative values in the canopy (up to -1.5). So in this
488 region close to flow separation and with strong direction shear the horizontal winds
489 show relatively little skewness, while vertical motion is dominated by strong down-
490 ward gusts from the upper canopy. The only other notable difference from skewness
491 profiles over flat ground are near canopy top at tower T3. For north-easterly cases
492 Sk_w becomes slightly positive above the canopy, while it remains negative for south-
493 westerly cases. In the south-westerly flow the tower is entirely within the separation
494 region and so strong downward events dominate. In contrast, for the north-easterly
495 cases the mean flow and other turbulent statistics profiles look similar to over flat
496 ground, and so this slight increase in strong upward motion events is somewhat sur-
497 prising.

498 **6 Conclusions**

499 A unique set of airflow measurements from within and above a forest canopy in
500 complex terrain has been presented. This dataset provides much needed information
501 to help support and improve our current understanding and modelling of canopy flows
502 over complex heterogeneous terrain.

503 Data from across-ridge flows have been presented and have been shown, at least
504 qualitatively, to be in agreement with predictions from idealized two-dimensional
505 theory, numerical models and wind-tunnel experiments. In particular the occurrence
506 of flow separation appears to be a common event in both south-westerly and north-
507 easterly flows, although the details of the separation are very dependent on local het-

508 erogeneities in the canopy cover and the terrain. Clearings in the canopy have been
509 seen to modify the wind profile and reduce or prevent the formation of flow separa-
510 tion, even at a short distance of order h into the clearing. Cases such as these have
511 highlighted the necessity to explicitly model the canopy and to capture the canopy
512 heterogeneity if models are to accurately predict flow patterns (including flow separa-
513 ration) over small-scale hills, or if comparison is to be made with observations made
514 in clearings. The occurrence of flow separation can also have significant effects on
515 scalar transport, as highlighted by Ross (2011) and so such details are also likely to be
516 important in the planning and interpretation of flux measurements at sites in complex
517 terrain.

518 The observed flow is strongly three dimensional with strong directional shear with
519 height in regions of flow separation. This has a significant impact on the Reynolds
520 stress terms $\overline{u'w'}$ and $\overline{v'w'}$ with $\overline{u'w'}$ being positive and $\overline{v'w'}$ being similar in mag-
521 nitude to $\overline{u'w'}$ at a number of locations, particularly for south-westerly flows with
522 larger-scale flow separation. This is something not seen in the many idealized two-
523 dimensional theoretical and modelling studies and makes interpretation of the flow
524 and direct comparison with simple theories complicated. The strong directional shear
525 may be important for wind damage to trees and for wind energy applications since
526 it may place additional torsional forces on the trees or wind turbines. Higher order
527 turbulence statistics show similarities with profiles over flat ground at some sites and
528 for some wind directions, but there are also significant differences, again particularly
529 around regions with strong directional shear.

530 In future this dataset will also offer useful opportunities to test the validity of the
531 turbulence closure schemes used in numerical models of canopy flow in complex and
532 heterogeneous terrain. It will also be important to validate the models themselves for
533 predicting flow in such conditions. Such validation beyond simple idealized problems
534 is essential if these models are to be used to understand complex canopy flows and to
535 make predictions of the impact of such flows.

536 **Acknowledgements** This work was funded by the Natural Environmental Research Council (NERC)
537 grant NE/C003691/1. ERG would like to acknowledge additional support through a NERC Collaborative
538 Award in Science and Engineering (CASE) award with Forest Research. We would like to thank Ian Brooks
539 and all those from the Universities of Leeds and Edinburgh, the Forestry Commission, Forest Research
540 and from the Met Office Research Unit at Cardington who loaned us equipment and assisted in the field
541 campaign.

542 **Appendix 1**

543 **References**

- 544 Allen T, Brown AR (2002) Large-eddy simulation of turbulent separated
545 flow over rough hills. *Boundary-Layer Meteorol* 102:177–198, DOI
546 10.1023/A:1013155712154
- 547 Ayotte KW, Davy RJ, Coppin PA (2001) A simple temporal and spatial analysis of
548 flow in complex terrain in the context of wind energy modelling. *Boundary-Layer*
549 *Meteorol* 98:275–295, DOI 10.1023/A:1026583021740
- 550 Baldocchi D, Falge E, Gu LH, Olson R, Hollinger D, Running S, Anthoni P, Bern-
551 hofer C, Davis K, Evans R, Fuentes J, Goldstein A, Katul G, Law B, Lee XH,

Instrument make and model	Use	Accuracies
3-D sonic anemometer: Metek USA-1	Four on towers T1 and T3, two at lower heights on tower T2	At 1 m s^{-1} : $\pm 0.1\text{ m s}^{-1}$ and $\pm 5^\circ$. At 4 m s^{-1} : $\pm 0.15\text{ m s}^{-1}$ and $\pm 3^\circ$. At 10 m s^{-1} : $\pm 0.3\text{ m s}^{-1}$ and $\pm 2^\circ$. For $20 - 50\text{ m s}^{-1}$: $\pm 2\%$ and $\pm 2^\circ$.*
3-D sonic anemometer: Gill R3A	Two at upper heights on T2	Wind speed: $< 1\%$ rms, wind direction: $< \pm 1\%$ rms**
Cup anemometer: NRG Type 40	Towers and AWS	0.1 m s^{-1} within a range of 5 m s^{-1} to 25 m s^{-1}
Wind vane: NRG Type 200P	AWS	1%
Temperature sensor: Betatherm Series 1 thermistor	Towers and AWS	1% at 25°C
Pressure sensor: Intersema MS5534	AWS	$\pm 0.5\text{ hPa}$ at 25°C
Digital temperature sensor: Sensirion SHT1x	AWS	$\pm 0.5^\circ\text{C}$

Table 1 Overview of instruments used throughout the field campaign. *Accuracy applies for horizontal wind speeds. **Accuracy applies for wind speed $< 32\text{ m s}^{-1}$ and for wind incidence angles $\pm 20^\circ$ from the horizontal.

552 Malhi Y, Meyers T, Munger W, Oechel W, Paw U KT, Pilegaard K, Schmid H,
553 Valentini R, Verma S, Vesala T, Wilson K, Wofsy S (2001) FLUXNET: A new
554 tool to study the temporal and spatial variability of ecosystem-scale carbon diox-
555 ide, water vapor, and energy flux densities. Bull Amer Met Soc 82:2415–2434,
556 DOI 10.1023/A:1002497616547

Tower	Within canopy	Canopy description	Altitude (m)	Site description
T1	Yes	Dense Sitka spruce plantation (16.8 m)	170 ± 10	Located on south-west facing slope in a large clearing (approximately 40m ²). Tower located to the north-east of the clearing. Steep rocky outcrop (approximately 5 m tall) dropping off to west of tower.
T2	Yes	Dense Sitka spruce plantation (18.5 m)	165 ± 10	Located on summit of ridge in a small clearing (approximately 15m ²).
T3	Yes	Sitka spruce plantation upslope, mixed deciduous forest downslope (15.7 m).	110 ± 10	Located on north-east facing slope in a natural clearing, on significantly steeper terrain than T1 and T2.

Table 2 Summary of the main features of each tower site describing canopy, altitude and general terrain. The heights included in the canopy description are mean canopy heights calculated from the survey plots nearest each site.

- 557 Belcher SE, Hunt JCR (1998) Turbulent flow over hills and waves. *Annu Rev Fluid*
558 *Mech* 30:507–538, DOI 10.1146/annurev.fluid.30.1.507
- 559 Belcher SE, Jerram N, Hunt JCR (2003) Adjustment of a turbulent boundary
560 layer to a canopy of roughness elements. *J Fluid Mech* 488:369–398, DOI
561 10.1017/S0022112003005019
- 562 Belcher SE, Finnigan JJ, Harman IN (2008) Flows through forest canopies in com-
563 plex terrain. *Ecol Apps* 18:1436–1453, DOI 10.1890/06-1894.1
- 564 Bradley EF (1980) An experimental study of the profiles of wind speed, shearing
565 stress and turbulence at the crest of a large hill. *Q J R Meteorol Soc* 106:101–123,

AWS	Within canopy	Canopy description	Altitude (m)	Site description
ARA	Yes	Dense Sitka spruce plantation (14.5 m)	150 ± 5	Located on south-west facing slope, with a large clearing to the south-west and extending east.
ARB	Yes	Dense Sitka spruce plantation (17.6 m)	175 ± 5	Located approximately 30 m south-east of T1.
ARC	Yes	Dense Sitka spruce plantation to the north-east (18.6 m), no canopy to the south-west.	112 ± 5	Located on the south-west facing slope, at the edge of the plantation. Plantation to the north-east, open field to the south-west.
ARE	No	NA	230 ± 1	Out of the canopy, approximately 200 m north-west of the plantation edge, on the north-east facing slope.
ARF	Yes	Mixed canopy of Sitka spruce and hybrid larch (26.8 m)	135 ± 10	Located on the steep, north-west facing slope, directly downslope from T2, fully surrounded by canopy, though canopy less dense than further upslope.
ARG	Yes	Dense Sitka spruce plantation (20.2 m)	180 ± 10	Located approximately 50 m north of T2 in a small clearing (approximately 5 m ²).
ARH	Yes	Mixed canopy of Sitka spruce and western hemlock (27.0 m)	115 ± 10	Located on the steep, north-east facing slope approximately 30 m north of T3. Fully surrounded by canopy though less dense than further upslope.
ARJ	No	NA	8 ± 5	Located at the base of the ridge, on the coast, out of the canopy.
ARL	No	NA	13 ± 5	Located at the base of the ridge, out of the canopy, at a valley mouth, approximately 100 m inland from the sea.
ARN	No	NA	221 ± 1	Located on the ridge summit, out of the canopy on a small plateau.
ARP	No	NA	263 ± 1	Located on the ridge summit, out of the canopy, on the summit of a small hillock. Rocky outcrops to the north-east.
ARQ	No	NA	213 ± 1	Located on the north-east facing slope, out of the canopy.

Table 3 Summary of the main features of each AWS site describing canopy, altitude and general terrain.

The heights included in the canopy description are the height of the tree with the greatest diameter at breast

height recorded at the survey plot closest to each site.

566 DOI 10.1002/qj.49710644708

567 Brown AR, Hobson JM, Wood N (2001) Large-eddy simulation of neutral turbulent
568 flow over rough sinusoidal ridges. *Boundary-Layer Meteorol* 98:411–441, DOI
569 10.1023/A:1018703209408

570 Cassiani M, Katul GG, Albertson JD (2008) The effects of canopy leaf area den-
571 sity on airflow across forest edges: Large-eddy simulation and analytical results.
572 *Boundary-Layer Meteorol* 126:433–460, DOI 10.1007/s10546-007-9242-1

573 Dupont S, Brunet Y (2008) Edge flow and canopy structure: A large-eddy simulation
574 study. *Boundary-Layer Meteorol* 126:51–71, DOI 10.1007/s10546-007-9216-3

575 Dupont S, Patton EG (2012) Influence of stability and seasonal canopy changes on
576 micrometeorology within and above an orchard canopy: The CHATS experiment.
577 *Agric For Meteorol* 157:11–29, DOI 10.1016/j.agrformet.2012.01.011

578 Dupont S, Brunet Y, Finnigan JJ (2008) Large-eddy simulation of turbulent flow over
579 a forested hill: Validation and coherent structure identification. *Q J R Meteorol*
580 *Soc* 134:1911–1929, DOI 10.1002/qj.328

581 Finnigan JJ (2000) Turbulence in plant canopies. *Annu Rev Fluid Mech* 32:519–571,
582 DOI 10.1146/annurev.fluid.32.1.519

583 Finnigan JJ (2008) An introduction to flux measurements in difficult conditions. *Ecol*
584 *Apps* 18:1340–1350, DOI 10.1890/07-2105.1

585 Finnigan JJ, Belcher SE (2004) Flow over a hill covered with a plant canopy. *Q J R*
586 *Meteorol Soc* 130:1–29, DOI 10.1256/qj.02.177

587 Finnigan JJ, Brunet Y (1995) Turbulent airflow in forests on flat and hilly terrain. In:
588 Coutts MP, Grace J (eds) *Wind and trees*, Cambridge University Press, Cambridge,

- 589 UK, pp 3–40
- 590 Foken T, Wichura B (1996) Tools for quality assessment of surface-based flux mea-
591 surements. *Agric For Meteorol* 78:83–105, DOI 10.1016/0168-1923(95)02248-1
- 592 Gardiner B, Blennow K, Carnus JM, Fleischer P, Ingemarson F, Land-
593 mann G, Lindner M, Marzano M, Nicoll B, Orazio C, Peyron JL, Re-
594 viron MP, Schelhaas MJ, Schuck A, Spielmann M, Usbeck T (2010)
595 Destructive Storms in European Forests: Past and Forthcoming Impacts.
596 Final Report to European Commission DG Environment. Online, URL
597 <http://ec.europa.eu/environment/forests/fprotection.htm>
- 598 Gardiner B, Schuck A, Schelhaas MJ, Orazio C, Blennow K,
599 Nicoll B (eds) (2013) Living with Storm Damage to Forests:
600 What Science Can Tell Us 3. European Forest Institute, URL
601 http://www.efi.int/files/attachments/publications/efi_wsctu_3_final_net.pdf
- 602 Hanewinkel M, Cullmann D, Schelhaas M, Nabuurs GJ, Zimmermann N (2013) Cli-
603 mate change may cause severe loss in the economic value of European forest land.
604 *Nature Climate Change* 3:203–207, DOI doi:10.1038/nclimate1687
- 605 Hunt JCR, Leibovich S, Richards KJ (1988) Turbulent shear flow over low hills. *Q J*
606 *R Meteorol Soc* 114:1435–1470, DOI 10.1002/qj.49711448405
- 607 Irvine MR, Gardiner BA, Hill MK (1997) The evolution of turbulence across a forest
608 edge. *Boundary-Layer Meteorol* 84:467–496, DOI 10.1023/A:1000453031036
- 609 Justus CG, Hargreaves WR, Yalcin A (1976) Nationwide assessment of poten-
610 tial output from wind-powered generators. *J Appl Meteor* 15:673–678, DOI
611 10.1175/1520-0450(1976)015<0673:NAOPOF>2.0.CO;2

- 612 Kaimal JC, Finnigan JJ (1994) Atmospheric boundary layer flows: their structure and
613 measurements. Oxford University Press, New York, USA
- 614 Lee X, Finnigan J, Paw U KT (2004) Coordinate systems and flux bias error. In:
615 Lee X, Massman W, Law B (eds) A handbook of micrometeorology: A guide for
616 surface flux measurements, Kluwer Academic Publishers, Dordrecht, The Nether-
617 lands, pp 33–66
- 618 Miller DR, Lin JD, Lu ZN (1991) Air flow across an alpine forest clearing: A model
619 and field measurements. *Agric For Meteorol* 56:209–225, DOI 10.1016/0168-
620 1923(91)90092-5
- 621 Morse AP, Gardiner BA, Marshall BJ (2002) Mechanisms controlling turbulence
622 development across a forest edge. *Boundary-Layer Meteorol* 103:227–251, DOI
623 10.1023/A:1014507727784
- 624 Neff DE, Meroney NR (1998) Wind-tunnel modelling of hill and vegetation influ-
625 ence on wind-power availability. *J Wind Eng Ind Aerodyn* 74:335–343, DOI
626 10.1016/S0167-6105(98)00030-0
- 627 Patton EG, Katul GG (2009) Turbulent pressure and velocity perturbations induced
628 by gentle hills covered with sparse and dense canopies. *Boundary-Layer Meteorol*
629 133:189–217, DOI 10.1007/s10546-009-9427-x
- 630 Poggi D, Katul GG (2007a) An experimental investigation of the mean momentum
631 budget inside dense canopies on narrow gentle hilly terrain. *Agric For Meteorol*
632 144:1–13, DOI 10.1016/j.agrformet.2007.01.009
- 633 Poggi D, Katul GG (2007b) Turbulent flows on forested hilly terrain: the recirculation
634 region. *Q J R Meteorol Soc* 133:1027–1039, DOI 10.1002/qj.73

- 635 Quine C, Gardiner BA (2007) Understanding how the interaction of wind and trees
636 results in windthrow, stem breakage and canopy gap formation. In: Johnson E,
637 Miyanishi K (eds) *Plant disturbance ecology: the process and the response*, Aca-
638 demic Press, Burlington, USA, pp 103–155
- 639 Raupach MR, Finnigan JJ, Brunet Y (1996) Coherent eddies and turbulence in vege-
640 tation canopies: the mixing length analogy. *Boundary-Layer Meteorol* 78:351–382,
641 DOI 10.1007/BF00120941
- 642 Romniger JT, Nepf HM (2011) Flow adjustment and interior flow associated
643 with a rectangular porous obstruction. *J Fluid Mech* 680:636–659, DOI
644 10.1017/jfm.2011.199
- 645 Ross AN (2008) Large eddy simulations of flow over forested ridges. *Boundary-*
646 *Layer Meteorol* 128:59–76, DOI 10.1007/s10546-008-9278-x
- 647 Ross AN (2011) Scalar transport over forested hills. *Boundary-Layer Meteorol*
648 141:179–199, DOI 10.1007/s10546-011-9628-y
- 649 Ross AN, Baker TP (2013) Flow over partially forested ridges. *Boundary-Layer Me-*
650 *teorol* 146, DOI 10.1007/s10546-012-9766-x
- 651 Ross AN, Vosper SB (2005) Neutral turbulent flow over forested hills. *Q J R Meteorol*
652 *Soc* 131:1841–1862, DOI 10.1256/qj.04.129
- 653 Ruck B, Adams E (1991) Fluid mechanical aspects of the pollutant transport to conif-
654 erous trees. *Boundary-Layer Meteorol* 56:163–195, DOI 10.1007/BF00119966
- 655 Vosper SB, Mobbs SD, Gardiner BA (2002) Measurements of the momentum budget
656 in flow over a hill. *Q J R Meteorol Soc* 128:2257–2280, DOI 10.1256/qj.01.11

-
- 657 Webster S, Brown AR, Cameron DR, Jones CP (2003) Improvements to the rep-
658 resentation of orography in the Met Office Unified Model. *Q J R Meteorol Soc*
659 129:1989–2010, DOI 10.1256/qj.02.133
- 660 Zeri M, Rebmann C, Feigenwinter C, Sedlak P (2010) Analysis of short periods
661 with strong and coherent CO₂ advection over a forested hill. *Agric For Meteo-*
662 *rol* 150(5):674–683, DOI 10.1016/j.agrformet.2009.12.003